Atomic Data Needs for X-ray Astronomy. 22 June 2000
http://heasarc.gsfc.nasa.gov/docs/heasarc/atomic/
M. A. Bautista, T. R. Kallman, and A. K. Pradhan, eds.

Modeling X-Ray Photoionized Plasmas: Ion Storage Ring Measurements of Low Temperature Dielectronic Recombination Rate Coefficients for L-Shell Iron

D. W. Savin[1], N. R. Badnell[2], T. Bartsch[3], C. Brandau[3], M. H. Chen[4], M. Grieser[5], G. Gwinner[5], A. Hoffknecht[3], S. M. Kahn[1], J. Linkemann[5], A. Müller[3], R. Repnow[5], A. A. Saghiri[5], S. Schippers[3], M. Schmitt[5], D. Schwalm[5], A. Wolf[5], and P. A. Závodszky[6]
[1]*Columbia Astrophysics Laboratory, Columbia University, New York, NY 10027, USA*
[2]*University of Strathclyde, Glasgow, G4 0NG, United Kingdom*
[3]*Institut für Kernphysik, Strahlenzentrum der Justus-Liebig-Universität, D-35392 Giessen, Germany*
[4]*Lawrence Livermore National Laboratory, Livermore, CA 94550, USA*
[5]*Max-Planck-Institut für Kernphysik, D-69117 Heidelberg, Germany*
[6]*National Superconducting Cyclotron Laboratory, Michigan State University, East Lansing, MI, 48824 USA*

Abstract. Iron L-shell ions (Fe XVII to Fe XXIV) play an important role in determining the line emission and thermal and ionization structures of photoionized gases. Existing uncertainties in the theoretical low temperature dielectronic recombination (DR) rate coefficients for these ions significantly affects our ability to model and interpret observations of photoionized plasmas. To help address this issue, we have initiated a laboratory program to produce reliable low temperature DR rates. Here we present some of our recent results and discuss some of their astrophysical implications.

1. Astrophysical Motivation

The ionization and heating of the media surrounding accretion-powered compact sources, such as active galactic nuclei (AGNs), X-ray binaries (XRBs), and cataclysmic variables, are dominated by photoionization. Theoretical models show that the ionization and thermal structures of these sources are determined by photoionization balanced by radiative recombination (RR) and dielectronic recombination (DR). These models also predict that the electron temperature at which an ion forms (Kallman et al. 1996) is far below the temperature at which the ion would form in coronal equilibrium (Mazzotta et al. 1998). Recent *ASCA* observations of the XRB Cyg X-3 have largely validated the predicted low temperatures (Liedahl and Paerels 1996). Under these conditions, low temperature DR is the dominant recombination channel for many ions.

Iron ions play an important role in determining the line emission and thermal and ionization structures of photoionized plasmas (Kallman et al. 1996; Hess et al. 1997; Savin et al. 1999). Of particular interest is L-shell iron (Fe XVII to Fe XXIV) which affects the range in parameter space over which photoionized gas is predicted to be thermally unstable (Hess et al. 1997; Savin et al. 1999). The need to better understand this instability has been demonstrated by recent *ASCA* observations of Cyg X-3. These observations have detected line emission from ions of neon, magnesium, silicon, and sulfur which are predicted to form in the region of thermal instability (Liedahl and Paerels 1996). With the recent launches of *Chandra* and *XMM*, many more observations are expected of line emission from ions predicted to form in thermally unstable photoionized plasmas.

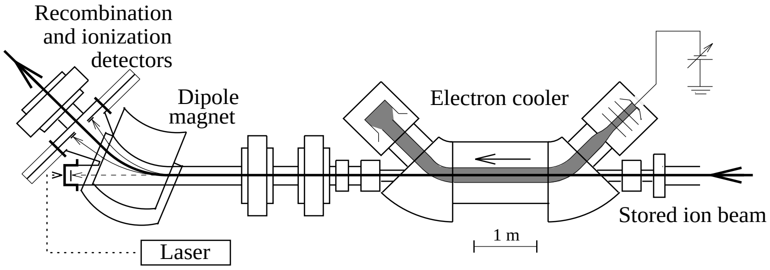

Figure 1. Shown is a partial overview of the TSR experimental arrangement for electron-ion collision measurements. Stored ions enter from the right. The electrons are merged with the ions and travel co-linear with them for ~ 1.5 m after which the electrons are separated from the ions. The ions then travel into a dipole magnet where recombined (ionized) ions are bent less (more) strongly than the primary beam and directed onto a particle counting detector.

2. Experimental Program

"The lack of reliable low temperature DR rates for most third row and higher elements is the dominant uncertainty in the ionization balance in photoionization equilibrium" (Ferland et al. 1998). Low temperature DR rates are theoretically and computationally challenging. There can be up to a factor of 2 spread between different calculated rates (Savin et al. 1999).

To address the needs for modeling X-ray photoionized plasmas, we have initiated a laboratory program to produce reliable low temperature DR rate coefficients for the L-shell iron ions. Measurements are carried out using the heavy-ion test storage ring (TSR) (Habs et al. 1989). To date we have carried out measurements of low temperature (*i.e.*, low collision energy) DR onto Fe XVIII (Savin et al. 1999; Savin et al. 1997), Fe XIX (Savin et al. 1999), Fe XX, Fe XXI, and Fe XXII.

DR is a two-step electron-ion recombination process which begins when a free electron collisionally excites an ion, via an $nl_j \rightarrow n'l'_{j'}$ excitation of a bound core electron, and is simultaneously captured. DR is complete when this state emits a photon which reduces the energy of the recombined ion to below its ionization limit. Low energy DR involves a $\Delta n \equiv n' - n = 0$ excitation of the core electron.

Storage rings are uniquely suited for their ability to study low energy DR of highly charged ions (Müller and Wolf 1997). Common laboratory techniques for measuring DR such as electron beam ion traps (Beiersdorfer et al. 1992) and tokamak plasmas (Bitter et al. 1993) can produce the desired ions, but cannot simultaneously reach the required low energies. Crossed electron-ion beam techniques cannot achieve the required low relative velocities (Müller et al. 1987; Savin et al. 1996). Single-pass, merged electron-ion beam techniques can achieve the desired low collision energies (Andersen et al. 1992). However, analysis of such data, particularly for ions with partially-filled shells, is usually complicated by the presence of an unknown quantity of metastable ions in the ion beam. Storage ring measurements overcome this problem by storing the ions long enough for all metastable levels to decay radiatively to the ground state.

Figure 1 shows a schematic of the portion of TSR used to perform DR experiments. Measurements are carried out by merging the ion and electron beams in one of the straight sections of TSR. After demerging, any recombined ions are magnetically separated from the stored ions and directed onto a detector. The relative electron-ion collision energy can be precisely controlled (from 0 eV to ~ 2000 eV) and the recombination signal measured as a function of this energy. The experiments basically follow the procedure described in Kilgus et al. (1992), Lampert et al. (1996). The accuracy of the measured DR resonance strengths is estimated to be better than 20%.

Recombination involves capturing a free electron into a Rydberg level n. Between the cooler and the dipole magnet, some of these captured electrons radiatively decay to lower-lying Rydberg levels. Recombined ions where the captured electron, at the dipole magnet, is in a level $n \gtrsim n_{max}$ are field ionized by the magnet and not detected. For TSR measurements of L-shell iron, n_{max} is typically ~ 120. Theoretical calculations indicate that the contributions to the total L-shell iron, low temperature DR rate coefficient from levels $n > n_{max}$ is $\lesssim 4\%$. DR rate coefficients derived from the experimentally measured DR resonance strengths are estimated to have an accuracy of better than 20%.

Experimental work has demonstrated that DR is sensitive to external electric and magnetic fields (Müller et al. 1987; Savin et al. 1996; Bartsch et al. 1997; Bartsch et al. 1999). However, in TSR the fields are extremely well controlled and we are able to carry out essentially field-free DR measurements. In the interaction region in TSR, external electric fields are insignificant ($E \lesssim 10$ V cm^{-1}). The ions also travel parallel to the magnetic field which confines the electrons and hence experience no $\mathbf{v} \times \mathbf{B}$ electric field. In addition, $\Delta n = 0$ DR measurements on lithium-like chlorine have shown that for DR into levels $n \lesssim 80$, field effects are not discernible at electric fields $E \lesssim 15$ V cm^{-1} (Bartsch et al. 1999). Our work here involves DR measurements for ions more highly charged than lithium-like chlorine, and the effect of external fields on the $\Delta n = 0$ DR process is predicted to decrease with increasing charge (Griffin and Pindzola 1987). Also, theoretical calculations indicate that the contributions to the total L-shell iron, low temperature DR rate coefficient from levels $n > 100$ is $\lesssim 10\%$ (Savin et al. 1999). Therefore, we expect external fields to have an insignificant effect on the L-shell iron low temperature DR rates derived from TSR data.

3. Recent Results

In Figure 2 we show preliminary data for $\Delta n = 0$ DR onto nitrogen-like Fe XX and boron-like Fe XXII. These data clearly demonstrate the resonance nature of the DR process. Following the procedures outlined in Savin et al. (1999), Kilgus et al. (1992), Lampert et al. (1996), we can fit the DR resonances to extract the relevant resonance strengths and energies. We then integrate the measured resonances with a Maxwellian electron velocity distribution to yield a total $\Delta n = 0$ DR rate coefficient for plasma modeling (cf., Savin et al. 1999; Savin et al. 1997; Savin 1999).

In Figure 3 we show our experimentally derived rate coefficient for $\Delta n = 0$ DR onto Fe XVIII and Fe XIX (Savin et al. 1999; Savin et al. 1997). We also show various theoretical DR rates published before our measurements were carried out as well as new calculations carried out using our measured Fe XVIII and Fe XIX resonance strength and energy measurements as benchmarks. Lastly, for comparison we have plotted the recommended RR rates.

For Fe XVIII and Fe XIX, the semi-empirical formula of Burgess (1965), the LS-coupling calculations of Roszman (1987a, 1987b), the intermediate coupling calculations of Dasgupta and Whitney (1990, 1994), and the multiconfiguration Dirac-Fock (MCDF) calculations of Chen (1988) all go rapidly to zero below $k_BT_e \sim 20$ eV. This is because these calculations were carried out for high temperature plasmas and have not included DR via $2p_{1/2} \to 2p_{3/2}$ core excitation channels (which is unimportant in high temperature plasmas). We also note here that LS-coupling does not include all possible autoionization channels which can contribute to the DR rate and thus should provide a lower limit to the true DR rate (Griffin et al. 1985; Badnell 1988).

Fe XVIII is predicted to peak in fractional abundance at $k_BT_e \sim 15$ eV in photoionized gas with cosmic abundances (Kallman et al. 1996). As a result, at the relevant temperatures in photoionized gas, the published rates underestimate needed DR rate by a factor of 2 to orders of magnitude.

At temperatures where the $2p_{1/2} \to 2p_{3/2}$ DR channel is unimportant, our derived rate coefficient is in best agreement with the Burgess formula and the results of Dasgupta & Whitney. As discussed in Savin et al. (1999), this agreement is almost definitely fortuitous. Agreement is poor with the LS-coupling calculations of Roszman which lie above our DR rate. The more sophisticated 1988 MCDF calculations of Chen (1988), which more correctly account for autoionization, are also in poor agreement with the experimental rate. At plasma temperatures $k_BT_e > 100$ eV, $\Delta n = 1$ DR begins to dominate the DR process (Chen 1988).

Fe XIX is predicted to peak in fractional abundance at $k_BT_e \sim 70$ eV in photoionized gas with cosmic abundances (Kallman et al. 1996). At this temperature the published calculations all lie above the experimentally derived rate.

For both Fe XVIII and Fe XIX, recent MCDF and multiconfiguration Breit-Pauli (MCBP) are in much better agreement with our experimental results than are previously published rates. The MCBP rates are not shown in Figure 3 but are in good agreement with the MCDF rates. However, we note

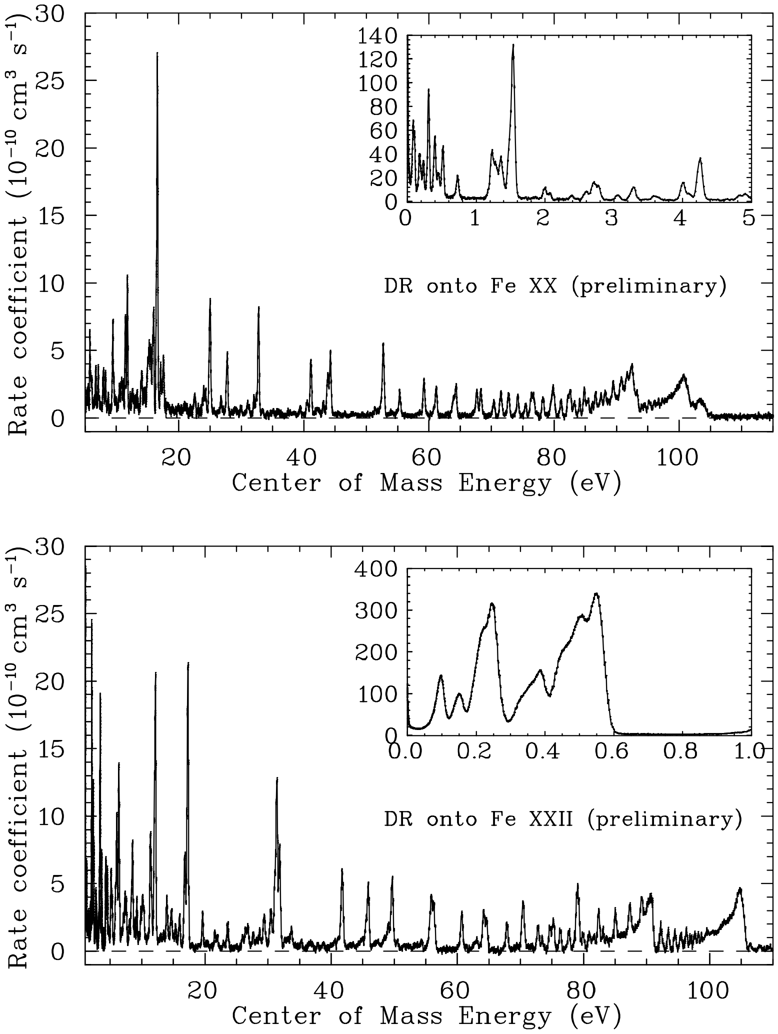

Figure 2. Preliminary data for $\Delta n = 0$ DR onto nitrogen-like Fe XX and boron-like Fe XXII. The measured rate coefficients represent the DR cross sections convolved with the experimental energy spread. The "background" is due primarily to RR with some residual signal due to charge transfer of the ions off rest gas in TSR.

that for Fe XVIII the new theory lies $\sim$ 35% below the experimental rate at $k_B T_e \sim 10$ eV. And for Fe XIX the new theory lies $\sim$ 30% above the experimental rate.

It is also worthwhile to point out that the theoretical results for Fe XVIII and Fe XIX from Roszman (1987a) and from Dasgupta and Whitney (1990) are for DR onto the ^{2}P and ^{3}P states, respectively. The results for Fe XVIII from Chen (1988) are for the $^2P_{3/2}$ state, as are our new MCDF and MCBP calculations. For Fe XIX our new calculations are for the $^3P_2$ state. At low temperatures, DR rate coefficients for different fine-structure states can be very different (Chen 1988) due to differences in resonance energies.

We can draw a number of conclusions from our experimental work to date. First, given the factor of $\sim$ 2 scatter between published $\Delta n = 0$ DR rates, we can infer that a similar uncertainty exists for published low temperature DR rates onto Fe XX through Fe XXIV. It is a goal of our research to produce reliable, experimentally derived DR rates to remove this uncertainty. Second, it is not possible to tell, in the absence of laboratory measurements, whether a theoretical DR rate lies above or below the "true"

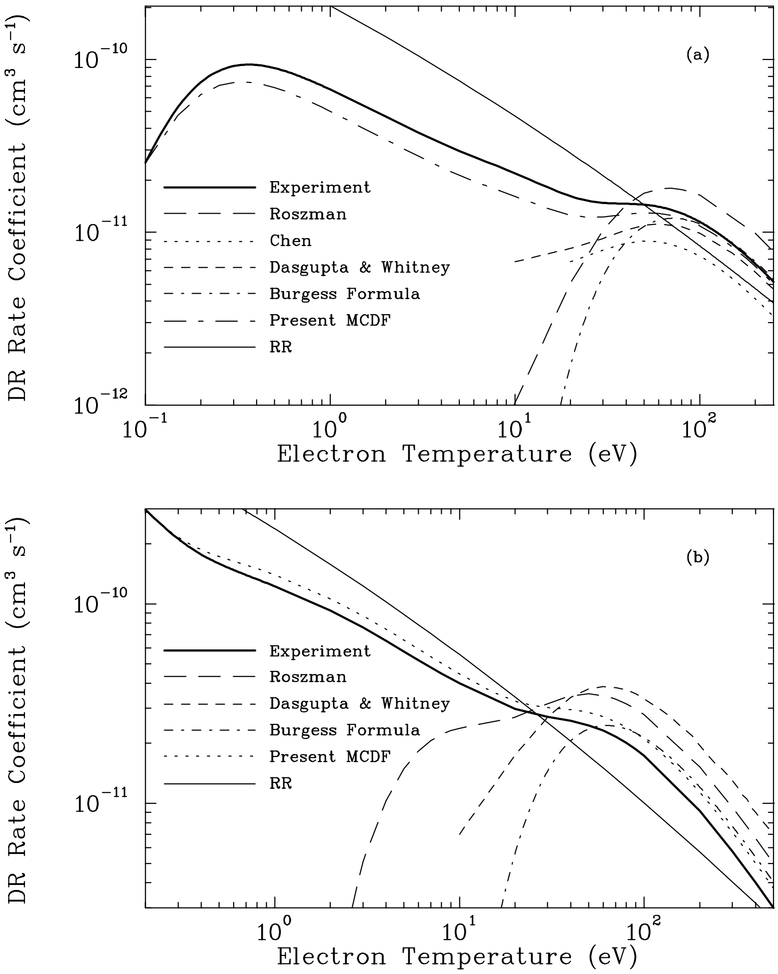

Figure 3. $\Delta n = 0$ DR rates for (a) Fe XVIII to Fe XVII and (b) Fe XIX to Fe XVIII (Savin et al. 1999). The thick solid curve shows the experimentally derived rates. The dotted-long-dashed curve in (a) and the dotted curve in (b) show our new MCDF calculations of Ref. (Savin et al. 1999). Not shown are our new MCBP calculations of Savin et al. (1999) which agree well with the MCDF calculations. The thin solid curve shows the recommended RR rate of Arnaud and Raymond (1992). The other curves show DR rates published before the measurements were carried out. See text for more details.

DR rate, nor by how much. Third, published DR rates do not necessarily provide reliable upper and lower limits to the value of the DR rate. Lastly, measurements of the relevant DR resonance strengths and energies are the only reliable way to verify the accuracy of DR calculations.

4. Astrophysical Implications

There are a number of potential astrophysical implications of our work to date. For example, DR via $2p_{1/2} \rightarrow 2p_{3/2}$ core excitations offers the possibility of new electron temperature and density diagnostics (Savin et al. 1998). Also, the estimated factor of 2 uncertainty in the published $\Delta n = 0$ DR rates for L-shell iron can dramatically affect the range in parameter space over which photoionized gas is thermally unstable, making it smaller or larger. However, the uncertainty in these DR rates cannot

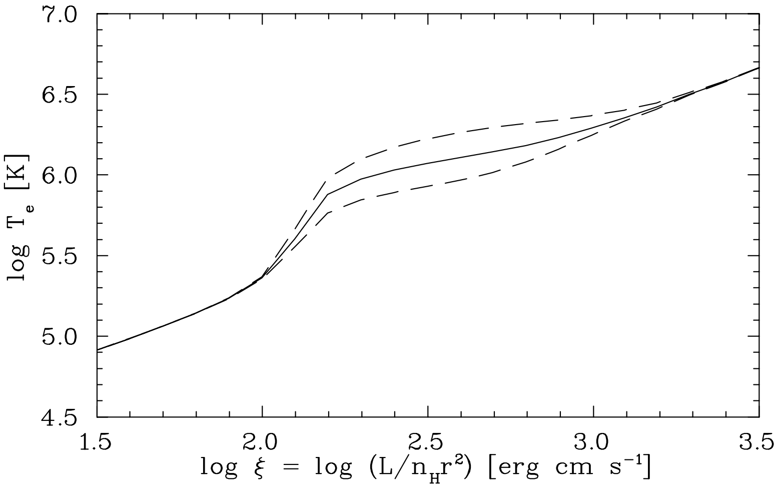

Figure 4. Predicted electron temperature versus ionization parameter ξ for a model AGN ionizing spectrum illuminating a slab of gas with cosmic abundances. The middle curve shows the predicted T_e using our experimentally derived $\Delta n = 0$ DR rates for Fe XVIII and Fe XIX and the unchanged $\Delta n = 0$ DR rates for Fe XX through Fe XXIV. The upper (lower) dashed curve shows our results when the $\Delta n = 0$ DR rates for Fe XX through Fe XXIV are increased (decreased) by a factor of 2.

remove the instability (Savin et al. 1999). Here we will only discuss the implications for line emission from photoionized gas.

We have used XSTAR (version 1.40b; Kallman and Krolik 1997) to investigate the effects on the temperature structure and line emission of photoionized gas due to our estimated factor of 2 uncertainty in the $\Delta n = 0$ DR rates onto Fe XX through Fe XXIV. We have run XSTAR with the relevant $\Delta n = 0$ DR rates unchanged, increased by a factor of two, and decreased by a factor of two. We assume cosmic abundances; and a model AGN ionizing spectrum with a photon number power law of $N \propto E^{-1.8}$ extending from 13.6 eV to 40 keV. Here E is the photon energy. More details are given in Savin et al. (1999).

Figure 4 shows the predicted electron temperature versus ionization parameter $\xi = L/n_H r^2$, where L is the luminosity of the ionizing source, n_H is the hydrogen nucleus density, and r is the distance from the ionizing source. Should a future observation yield a $\log T_e \sim 6.1$ (where T_e is in K), then the uncertainty in the inferred ξ would be a factor of ~ 3.4. For observations in this range of ξ, this uncertainty will hamper our ability to determine L or n_H to within a factor of ~ 3.4 or r to a factor of ~ 1.8.

The estimated uncertainty in the DR rates results, for a given value of ξ, in as much as a factor of ~ 1.8 variation between the predicted electron temperatures. The spectroscopic implications of this temperature uncertainty are shown in Figure 5. Here we have used XSTAR to produce synthetic spectra which we have folded through the *XMM* Reflection Grating Spectrometer (RGS) using XSPEC. The dramatic difference between the two spectra in Figure 5 is due to the different temperatures for the two test cases. The temperature dramatically affects the width of the radiative recombination continua seen in the spectra and in the line-to-continuum ratios.

Acknowledgments. We thank the staff and technicians of the TSR group for support during the beam time. We also thank A. Rasmussen for providing the *XMM*-RGS response matrix for the synthetic spectra. This work was supported in part by NASA High Energy Astrophysics X-Ray Astronomy Research and Analysis grant NAG5-5123. Travel and living expenses for DWS were supported by NATO Collaborative Research Grant CRG-950911. The experimental work has been supported in part by the German Federal Minister for Education, Science, Research, and Technology (BMBF) under Contract Nos. 06 GI 475, 06 GI 848, and 06 HD 854I. Work performed at Lawrence Livermore National Laboratory was under the auspices of the US Department of Energy (contract number W-7405-ENG-48).

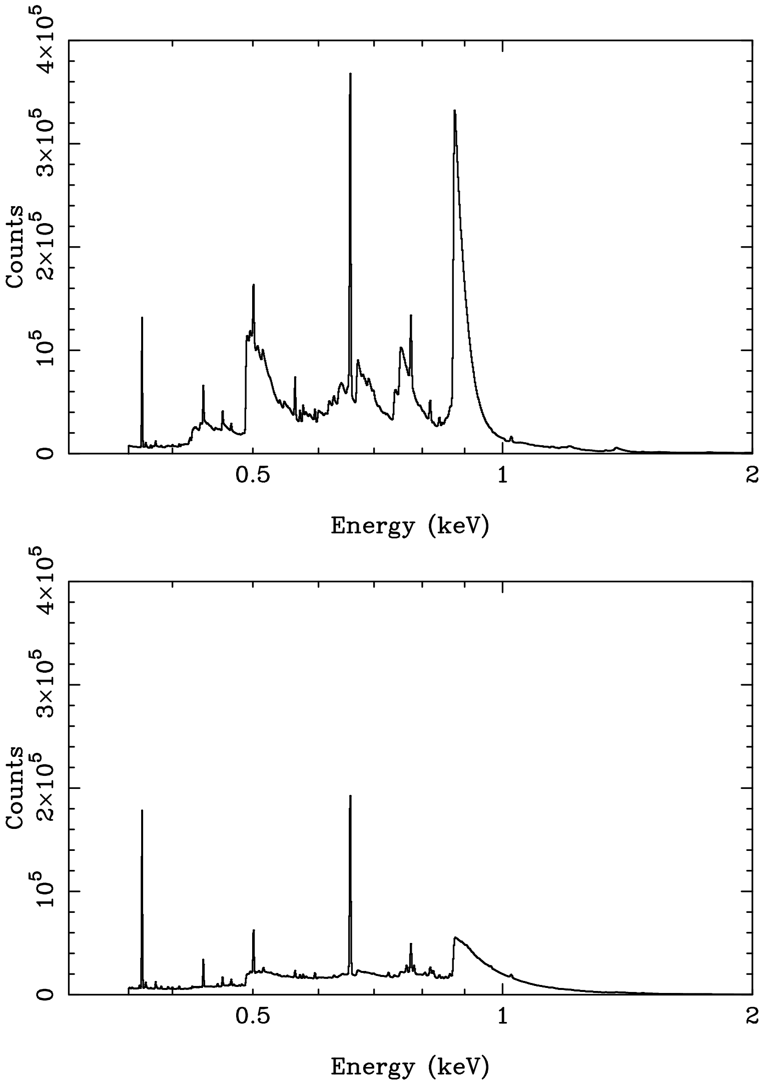

Figure 5. Synthetic spectra using XSTAR for a slab of photoionized gas with cosmic abundances at $\log \xi \sim 2.138$. The spectra have been folded through the *XMM*-RGS response matrix using XSPEC. We use our experimentally derived $\Delta n = 0$ DR rates for Fe XVIII and Fe XIX. The Fe XIX through Fe XXIV $\Delta n = 0$ DR rates have been decreased (increased) by a factor of 2 for the spectrum on the left (right).

References

Andersen, L. H., Pan, G.-Y., Schmidt, H. T., Pindzola, M. S., and Badnell, N. R. 1992, Phys. Rev. A 45, 6332.

Arnaud, M., and Raymond, J. C.1992, Astrophys. J. 398, 394.

Badnell, N. R. 1988, J. Phys. B 21, 749.

Bartsch, T., Müller, A., Spies, W., Linkemann, J., Danared, H., DeWitt, D. R., Gao, H., Zong, W., Schuch, R., Wolf, A., Dunn, G. H., Pindzola, M. S., and Griffin, D. C. 1997, Phys. Rev. Lett. 79, 2233.

Bartsch, T., Schippers, S., Müller, A., Brandau, C., Gwinner, G., Saghiri, A. A., Beutelspacher, M., Grieser, M., Schwalm, D., Wolf, A., Danared, H., and Dunn, G. H. 1999, Phys. Rev. Lett. 82, 3779.

Beiersdorfer, P., Phillips, T. W., Wong, K. L., Marrs, R. E., Vogel, D. A. 1992, Phys. Rev. A 46, 3812.

Bitter, M., Hsuan, H., Hill, K. W., and Zarnstorff, M., 1993, Phys. Scr. T47, 87.

Burgess, A.1965, Astrophys. J. 141, 1588.

Chen, M. H. 1988, Phys. Rev. A 38, 2332.

Dasgupta, A., and Whitney, K. G. 1990, Phys. Rev. A 42, 2640.

Dasgupta, A., and Whitney, K. G. 1994, At. Data Nucl. Data Tables 58, 77.

Ferland, G. J., Korista, K. T., Verner, D. A., Ferguson, J. W., Kingdon, J. B., and Verner, E. M. 1998, Publ. Astron. Soc. Pacific 110, 761.

Griffin, D. C., Pindzola, M. S. 1987, Phys. Rev. A 35, 2821.

Griffin, D. C., Pindzola, M. S., and Bottcher, C. 1985 Phys. Rev. A 31, 568.

Habs, D. et al. 1989, Nucl. Instrum. Methods B43, 390.

Hess, C. J., Kahn, S. M., and Paerels, F. B. S. 1997, Astrophys. J. 478, 94.

Kallman, T. R., Liedahl, D., Osterheld, A., Goldstein, W., and Kahn, S. 1996, Astrophys. J. 465, 994.

Kallman, T. R., and Krolik, J. H. 1997, XSTAR, A Spectral Analysis Tool. The XSTAR code and related documentation is available at ftp://legacy.gsfc.nasa.gov/software/plasma_codes/xstar/.

Kilgus, G., Habs, D., Schwalm, D., Wolf, A, Badnell, N. R., and Müller, A. 1992, Phys. Rev. A 46, 5730.

Lampert, A., Wolf, A., Habs, D., Kilgus, G., Schwalm, D., Pindzola, M. S., and Badnell, N. S. 1996, Phys. Rev. A 53, 1413.

Liedahl, D. A., and Paerels, F. 1996, Astrophys. J. Lett. 468, L33.

Mazzotta, P., Mazzitellie, G., Colafrancesco, S., and Vittorio, N. 1998, Astron. Astrophys. Suppl. Ser. 133, 403.

Müller, A., Belić, D. S., DePaola, B. D., Djurić, N., Dunn, G. H., Mueller, D. W., and Timmer, C. 1987, Phys. Rev. A 36, 599.

Müller, A., and Wolf, A. 1997, in "Accelerator-Based Atomic Physics Techniques and Applications", ed. S. M. Shafroth, and J. C. Austin (AIP: New York), p. 147.

Roszman, L. J. 1987a, Phys. Rev. A 35, 2138.

Roszman, L. J. 1987b, Phys. Rev. A 35, 3368.

Savin, D. W. 1999, Astrophys. J. 523, 855.

Savin, D. W., Bartsch, T., Chen, M. H., Kahn, S. M., Liedahl, D. A., Linkemann, J., Müller, A., Schippers, S., Schmitt, M., Schwalm, D., and Wolf, A. 1997, Astrophys. J. Lett. 489, L115.

— 1998, in "NIST Special Publication 926, Poster Papers, International Conference on Atomic and Molecular Data and Their Applications (ICAMDATA 97)", ed. W. L. Wiese and P. J. Mohr, Washington, D.C.: U.S. Government Printing Office, p. 96.

Savin, D. W., Gardner, L. D., Reisenfeld, D. B., Young, A. R., and Kohl, J. L. 1996, Phys. Rev. A 53, 280.

Savin, D. W., Kahn, S. M., Grieser, M., Linkemann, J., Repnow, R., Saghiri, A. A., Schmitt, M., Schwalm, D., Wolf, A., Bartsch, T., Brandau, C., Hoffknecht, A.,Müller, A., Schippers, S., Chen, M. H., and Badnell, N. R. 1999, Astrophys. J. Suppl. Ser. 123, 687.